

Fig. 2 GSEA evaluation associated with SLC22A7: **a** mitochondrion ($P = 0.008$; FDR = 0.199; NES = 1.804), **b** oxidoreductase activity ($P = 0.006$; FDR = 0.157; NES = 1.854), and **c** fatty acid metabolic

process ($P = 0.021$; FDR = 0.177; NES = 1.723). **d** Low expression of sirtuin 3 was associated with a poor prognosis ($P = 0.018$)

albumin levels, which were recognized as risk factors for the occurrence of HCC in univariate analyses of the training set (Table 3), did not decide the clinical outcome in the multicenter validation study (Table 4). Multivariate analysis of the training set and the validation study revealed the low SLC22A7 expression to be the only

reliable factor for predicting MO of HCC. The correlation between SLC22A7 gene expression and platelet counts were 0.167 ($P = 0.246$), and 0.134 ($P = 0.355$), respectively (data not shown). There was no difference in SLC22A7 expression between virus negative patients, HBV positive patients and HCV positive patients

($P = 0.439$). The SLC22A7 expression may be independent of platelet count and serum albumin decrease, predicting another aspect of liver functional reserve.

The precise indicator derived from noncancerous liver tissue determined the prognosis, which was not governed by tumor progression. According to the genome-wide gene expression analysis in the training set (Table 1), SLC22A7 best determined the clinical outcome in the organic anion transporter genes (GO:0015711), as judged by Cox regression analysis in ($P = 0.001$). Figure 1a shows the significant difference in tumor-free survival after hepatectomy according to SLC22A7 expression ($P = 0.001$).

The information obtained in the training set was validated in a prospective multicenter study using tissue microarrays (Fig. 1b). To this end, low SLC22A7 expression certainly determined MFS (Table 4). Regarding occurrence-free survival in the present study, de novo HCC may occur at 1 year after hepatectomy in patients with low SLC22A7 expression (Fig. 1). In this context, the prognostic curves appeared to be compatible with clinical observations. Anatomic resection did not decrease the risk for MFS in the multicenter study. It is reasonable that anatomic resection is not available in noncancerous liver with low SLC22A7 expression promoting de novo HCC. The aforementioned criteria were enough to determine the MO of HCC, since the anatomic resection prevents local recurrence within Milan criteria.

Whether oxidative stress resulting from reactive oxygen species in noncancerous tissue or cellular mitochondrial dysfunction promotes hepatocarcinogenesis has been discussed [18, 19]. Antioxidants such as glutathione play an important role and serve as essential components of the detoxification mechanism [9]. Our previous study identified CYP1A2 as an index for HCC recurrence [18]. The CYP1A2 expression is significantly decreased in the steatotic liver induced with orotic acid [20, 21]. The CYP1A2 and SLC22A7 are regulated by interferon-alpha 2b in human primary hepatocytes [22]. Interferon-alpha 2b induced partial remission of hepatoma [23]. These reports imply the possibility that CYP1A2 and SLC22A7 down regulation, are an early alert symptom of MO. In this aspect, decreased SLC22A7 expression may serve as a reliable surrogate biomarker for the prognosis and treatment of HCC.

Organic anion transporters are responsible for the uptake and exclusion of xenobiotics and organic anions [24, 25]. Serum organic anions and xenobiotics are emptied into the Disse's space, taken up by transporters at the hepatocellular sinusoidal membrane, and detoxified in the cytoplasm [26, 27]. The SLC22A7 expressed on the hepatocellular sinusoidal membrane takes up orotic acid [11]. Orotic acid has been regarded as a promoter of liver carcinogenesis, although the detailed mechanisms are unknown [28–30].

Moreover, mitochondrial sirtuin 3 may be involved in the metabolic cycle of orotic acid. Sirtuin 3, by regulating OTC activity to decrease orotic acid, inhibits hepatocellular carcinoma cell growth [31]. Previous research reported that exposure to orotic acid after hepatectomy promotes liver carcinogenesis [12]. Orotic aciduria and encephalopathy were observed in HCC patients without liver cirrhosis [32]. We focused on Sirtuin 3 regulating orotic acid production, because SLC22A7 transports orotic acids. Sirtuin 3 was reported as the regulator of mitochondrial metabolism and the inhibitor of hepatocellular carcinoma cell growth. The present findings indicate that the decreased sirtuin3 expression coinciding with decreased SLC22A7 may regulate hepatocellular orotic acid concentrations to promote MO of HCC (Fig. 2d). The gene expression levels of SLC22A7 correlated with that of sirtuin3. Furthermore, the customized sirtuin 3-related gene set revealed significant correlation with SLC 22A7 expression (Supplementary Figs. 2, 3).

In conclusion, the down regulation of SLC22A7 in noncancerous liver tissue may have promoted the MO of early-stage HCC in the training and multicenter validation studies. Evaluating SLC22A7 expression may be useful for selecting treatment strategies. Further research is required to determine whether the hepatocellular mechanisms involving mitochondrial metabolism increase hepatocellular liver carcinogenesis. Such studies could address whether antioxidant therapy or another therapy to prevent hepatocarcinogenesis would become available in patients with low SLC22A7 expression.

Acknowledgments This work was supported by a Health and Labour Sciences Research Grant (H20-Kanen-Ippan-001) from the Ministry of Health, Labour, and Welfare of Japan and a Grant-in Aid for Scientific Research from the Ministry of Education, Culture, Sports, Science, and Technology of Japan. The authors thank Hiromi Ohnari and Ayumi Shioya for clerical and technical assistance.

Conflict of interest The authors declare that they have no conflict of interest.

References

1. Yang JD, Roberts LR. Hepatocellular carcinoma: a global view. *Nat Rev Gastroenterol Hepatol*. 2010;7:448–58.
2. Schlitt HJ, Schnitzbauer AA. Hepatocellular carcinoma: agents and concepts for preventing recurrence after curative treatment. *Liver Transpl*. 2011;17(Suppl 3):S10–2.
3. Utsunomiya T, Shimada M, Imura S, Morine Y, Ikemoto T, Mori M. Molecular signatures of noncancerous liver tissue can predict the risk for late recurrence of hepatocellular carcinoma. *J Gastroenterol*. 2010;45:146–52.
4. Japan LCSGo: The general rules for the clinical and pathological study of primary liver cancer (in Japanese). 5th ed. Tokyo: Kanehara; 2009. p. 43.

5. Arii S, Yamaoka Y, Futagawa S, Inoue K, Kobayashi K, Kojiro M, et al. Results of surgical and nonsurgical treatment for small-sized hepatocellular carcinomas: a retrospective and nationwide survey in Japan. The liver cancer study group of Japan. *Hepatology*. 2000;32:1224–9.
6. Hasegawa K, Kokudo N, Imamura H, Matsuyama Y, Aoki T, Minagawa M, et al. Prognostic impact of anatomic resection for hepatocellular carcinoma. *Ann Surg*. 2005;242:252–9.
7. Imamura H, Matsuyama Y, Tanaka E, Ohkubo T, Hasegawa K, Miyagawa S, et al. Risk factors contributing to early and late phase intrahepatic recurrence of hepatocellular carcinoma after hepatectomy. *J Hepatol*. 2003;38:200–7.
8. Kobayashi A, Miyagawa S, Miwa S, Nakata T. Prognostic impact of anatomical resection on early and late intrahepatic recurrence in patients with hepatocellular carcinoma. *J Hepatobiliary Pancreat Surg*. 2008;15:515–21.
9. Kudo A, Kashiwagi S, Kajimura M, Yoshimura Y, Uchida K, Arii S, et al. Kupffer cells alter organic anion transport through multidrug resistance protein 2 in the post-cold ischemic rat liver. *Hepatology*. 2004;39:1099–109.
10. Sekine T, Cha SH, Tsuda M, Apiwattanakul N, Nakajima N, Kanai Y, Endou H. Identification of multispecific organic anion transporter 2 expressed predominantly in the liver. *FEBS Lett*. 1998;12:179–82.
11. Fork C, Bauer T, Golz S, Geerts A, Weiland J, Del Turco D, et al. Oat2 catalyses efflux of glutamate and uptake of orotic acid. *Biochem J*. 2011;436:305–12.
12. Laconi E, Vasudevan S, Rao PM, Rajalakshmi S, Pani P, Sarma DS. The development of hepatocellular carcinoma in initiated rat liver after a brief exposure to orotic acid coupled with partial hepatectomy. *Carcinogenesis*. 1993;14:2527–30.
13. Takayama T, Makuuchi M, Hirohashi S, Sakamoto M, Yamamoto J, Shimada K, et al. Early hepatocellular carcinoma as an entity with a high rate of surgical cure. *Hepatology*. 1998;28:1241–6.
14. Enomoto A, Takeda M, Shimoda M, Narikawa S, Kobayashi Y, Yamamoto T, et al. Interaction of human organic anion transporters 2 and 4 with organic anion transport inhibitors. *J Pharmacol Exp Ther*. 2002;301:797–802.
15. Hallows WC, Yu W, Smith BC, Devries MK, Ellinger JJ, Someya S, et al. Sirt3 promotes the urea cycle and fatty acid oxidation during dietary restriction. *Mol Cell*. 2011;41:139–49.
16. Hirschey MD, Shimazu T, Goetzman E, Jing E, Schwer B, Lombard DB, et al. Sirt3 regulates mitochondrial fatty-acid oxidation by reversible enzyme deacetylation. *Nature*. 2010;464:121–5.
17. Hoshida Y, Villanueva A, Kobayashi M, Peix J, Chiang DY, Camargo A, et al. Gene expression in fixed tissues and outcome in hepatocellular carcinoma. *N Engl J Med*. 2008;359:1995–2004.
18. Tanaka S, Mogushi K, Yasen M, Ban D, Kudo A, Arii S, et al. Oxidative stress pathways in noncancerous human liver tissue to predict hepatocellular carcinoma recurrence: a prospective, multicenter study. *Hepatology*. 2011;54:1273–81.
19. Marra M, Sordelli IM, Lombardi A, Lamberti M, Tarantino L, Giudice A, et al. Molecular targets and oxidative stress biomarkers in hepatocellular carcinoma: an overview. *J Transl Med*. 2011;9:171.
20. Su GM, Sefton RM, Murray M. Down-regulation of rat hepatic microsomal cytochromes p-450 in microvesicular steatosis induced by orotic acid. *J Pharmacol Exp Ther*. 1999;291:953–9.
21. Zhang WV, Ramzan I, Murray M. Impaired microsomal oxidation of the atypical antipsychotic agent clozapine in hepatic steatosis. *J Pharmacol Exp Ther*. 2007;322:770–7.
22. Chen C, Han YH, Yang Z, Rodrigues AD. Effect of interferon-alpha2b on the expression of various drug-metabolizing enzymes and transporters in co-cultures of freshly prepared human primary hepatocytes. *Xenobiotica*. 2011;41:476–85.
23. Locker GJ, Mader RM, Steiner B, Wenzl E, Zielinski CC, Steger GG. Benefit of interferon-alpha2b in a patient with unresectable hepatoma and chronic infection with hepatitis c virus. *Eur J Gastroenterol Hepatol*. 2000;12:251–3.
24. Kudo A, Ban D, Aihara A, Irie T, Ochiai T, Nakamura N, Tanaka S, Arii S. Decreased Mrp2 transport in severe macrovesicular fatty liver grafts. *J Surg Res*. 2012;178(2):915–21.
25. Ban D, Kudo A, Sui S, Tanaka S, Nakamura N, Ito K, et al. Decreased mrp2-dependent bile flow in the post-warm ischemic rat liver. *J Surg Res*. 2009;153:310–6.
26. Norimizu S, Kudo A, Kajimura M, Ishikawa K, Taniai H, Suematsu M, et al. Carbon monoxide stimulates mrp2-dependent excretion of bilirubin-ixalpha into bile in the perfused rat liver. *Antioxid Redox Signal*. 2003;5:449–56.
27. Sui S, Kudo A, Suematsu M, Tanaka S, Ito K, Arii S, et al. Preservation solutions alter mrp2-dependent bile flow in cold ischemic rat livers. *J Surg Res*. 2010;159:572–81.
28. Rao PM, Nagamine Y, Roomi MW, Rajalakshmi S, Sarma DS. Orotic acid, a new promoter for experimental liver carcinogenesis. *Toxicol Pathol*. 1984;12:173–8.
29. Laurier C, Tatematsu M, Rao PM, Rajalakshmi S, Sarma DS. Promotion by orotic acid of liver carcinogenesis in rats initiated by 1,2-dimethylhydrazine. *Cancer Res*. 1984;44:2186–91.
30. Denda A, Laconi E, Rao PM, Rajalakshmi S, Sarma DS. Sequential histopathological analysis of hepatocarcinogenesis in rats during promotion with orotic acid. *Cancer Lett*. 1994;82:55–64.
31. Zhang YY, Zhou LM. Sirt3 inhibits hepatocellular carcinoma cell growth through reducing mdm2-mediated p53 degradation. *Biochem Biophys Res Commun*. 2012;423:26–31.
32. Jeffers LJ, Dubow RA, Zieve L, Reddy KR, Livingstone AS, Neimark S, et al. Hepatic encephalopathy and orotic aciduria associated with hepatocellular carcinoma in a noncirrhotic liver. *Hepatology*. 1988;8:78–81.

A small-molecule AdipoR agonist for type 2 diabetes and short life in obesity

Miki Okada-Iwabu^{1,2,3*}, Toshimasa Yamauchi^{1,2,3*}, Masato Iwabu^{1,2*}, Teruki Honma⁴, Ken-ichi Hamagami¹, Koichi Matsuda¹, Mamiko Yamaguchi¹, Hiroaki Tanabe⁴, Tomomi Kimura-Someya⁴, Mikako Shirouzu⁴, Hitomi Ogata⁵, Kumpei Tokuyama⁵, Kohjiro Ueki¹, Tetsuo Nagano⁶, Akiko Tanaka^{4,6}, Shigeyuki Yokoyama^{4,7} & Takashi Kadowaki^{1,2,3}

Adiponectin secreted from adipocytes binds to adiponectin receptors AdipoR1 and AdipoR2, and exerts antidiabetic effects via activation of AMPK and PPAR- α pathways, respectively. Levels of adiponectin in plasma are reduced in obesity, which causes insulin resistance and type 2 diabetes. Thus, orally active small molecules that bind to and activate AdipoR1 and AdipoR2 could ameliorate obesity-related diseases such as type 2 diabetes. Here we report the identification of orally active synthetic small-molecule AdipoR agonists. One of these compounds, AdipoR agonist (AdipoRon), bound to both AdipoR1 and AdipoR2 *in vitro*. AdipoRon showed very similar effects to adiponectin in muscle and liver, such as activation of AMPK and PPAR- α pathways, and ameliorated insulin resistance and glucose intolerance in mice fed a high-fat diet, which was completely obliterated in AdipoR1 and AdipoR2 double-knockout mice. Moreover, AdipoRon ameliorated diabetes of genetically obese rodent model *db/db* mice, and prolonged the shortened lifespan of *db/db* mice on a high-fat diet. Thus, orally active AdipoR agonists such as AdipoRon are a promising therapeutic approach for the treatment of obesity-related diseases such as type 2 diabetes.

The number of overweight individuals worldwide has grown markedly, leading to an escalation of obesity-related health problems associated with increased morbidity and mortality. Insulin resistance is a common feature of obesity and predisposes the affected individuals to a variety of pathologies, including type 2 diabetes and cardiovascular diseases. Although considerable progress has been made in understanding the molecular mechanisms underlying insulin resistance and type 2 diabetes, their satisfactory treatment modalities remain limited^{1–4}.

Adiponectin (*Adipoq*)^{5–8} is an antidiabetic and antiatherogenic adipokine. Plasma adiponectin levels are decreased in obesity, insulin resistance and type 2 diabetes⁹. Replenishment of adiponectin has been shown to ameliorate insulin resistance and glucose intolerance in mice^{10–12}. This insulin sensitizing effect of adiponectin seems to be mediated, at least in part, by an increase in fatty-acid oxidation via activation of AMP-activated protein kinase (AMPK)^{13–15} and also via peroxisome proliferator-activated receptor (PPAR)- α ^{16,17}.

We previously reported the expression cloning of complementary DNA encoding adiponectin receptors 1 and 2 (*AdipoR1* and *AdipoR2*)¹⁸. AdipoR1 and AdipoR2 are predicted to contain seven-transmembrane domains¹⁸, but to be structurally and functionally distinct from G-protein-coupled receptors¹⁹. AdipoR1 and AdipoR2 serve as the major receptors for adiponectin *in vivo*, with AdipoR1 activating the AMPK pathways and AdipoR2 activating the PPAR- α pathways²⁰.

In skeletal muscle²¹, AdipoR1 is predominantly expressed and activates AMPK²² and PPAR- γ coactivator (PGC)-1 α (ref. 23) as well as Ca²⁺ signalling pathways, which have also been shown to be activated by exercise^{24,25}. Exercise has been reported to have beneficial effects on obesity-related diseases such as type 2 diabetes, and could contribute to healthy longevity²⁶. Liver expresses AdipoR1 and AdipoR2, both of which have roles in the regulation of glucose and lipid metabolism,

inflammation, and oxidative stress *in vivo*²⁰. Here we report the discovery of an orally active synthetic small molecule that binds to and activates both AdipoR1 and AdipoR2, ameliorates insulin resistance and type 2 diabetes, and prolongs the shortened lifespan of *db/db* mice.

Identification of small-molecule agonists of AdipoR

To identify orally active compounds that could bind to and activate AdipoR, we screened a number of small molecules in the chemical library at Open Innovation Center for Drug Discovery, The University of Tokyo²⁷. We performed functional assays to determine the ability of small molecules to activate AMPK (Extended Data Table 1 and Extended Data Fig. 1) and to ascertain the dependency of small molecules on AdipoR in C2C12 myotubes by testing the effects of suppression of AdipoR expression by specific short interfering RNA (siRNA) on phosphorylation of AMPK stimulated with each compound (Extended Data Table 2 and Extended Data Fig. 2). We named one of these hits AdipoR agonist (AdipoRon; Fig. 1a). We also used compounds 112254 and 165073 in some of the experiments as another hit and a non-hit, respectively (Extended Data Tables 1 and 2 and Extended Data Figs 1 and 2).

The treatment of C2C12 myotubes with AdipoRon caused an increase in the phosphorylation of Thr 172 in the α -subunit of AMPK (α AMPK)²⁸. AdipoRon at concentrations of 5–50 μ M increased AMPK phosphorylation in a dose-dependent manner to almost the same extent as did adiponectin (Fig. 1b, c) without mitochondrial complex I inhibition (Extended Data Fig. 3a). Suppression of AdipoR1 by specific siRNA (Extended Data Fig. 3b, c) greatly reduced the increase in AMPK phosphorylation induced by AdipoRon (Fig. 1c), indicating that AdipoRon increased AMPK phosphorylation via AdipoR1. Compound number 112254 (another hit) also significantly increased phosphorylation of

¹Department of Diabetes and Metabolic Diseases, Graduate School of Medicine, The University of Tokyo, Tokyo 113-0033, Japan. ²Department of Integrated Molecular Science on Metabolic Diseases, 22nd Century Medical and Research Center, The University of Tokyo, Tokyo 113-0033, Japan. ³Department of Molecular Medicinal Sciences on Metabolic Regulation, 22nd Century Medical and Research Center, The University of Tokyo, Tokyo 113-0033, Japan. ⁴RIKEN Systems and Structural Biology Center, Tsurumi, Yokohama 230-0045, Japan. ⁵Graduate School of Comprehensive Human Sciences, University of Tsukuba, Tsukuba 305-8577, Japan. ⁶Open Innovation Center for Drug Discovery, The University of Tokyo, 7-3-1 Hongo, Bunkyo-ku, Tokyo 113-0033, Japan. ⁷Graduate School of Science, The University of Tokyo, Bunkyo-ku, Tokyo 113-0033, Japan.

*These authors contributed equally to this work.

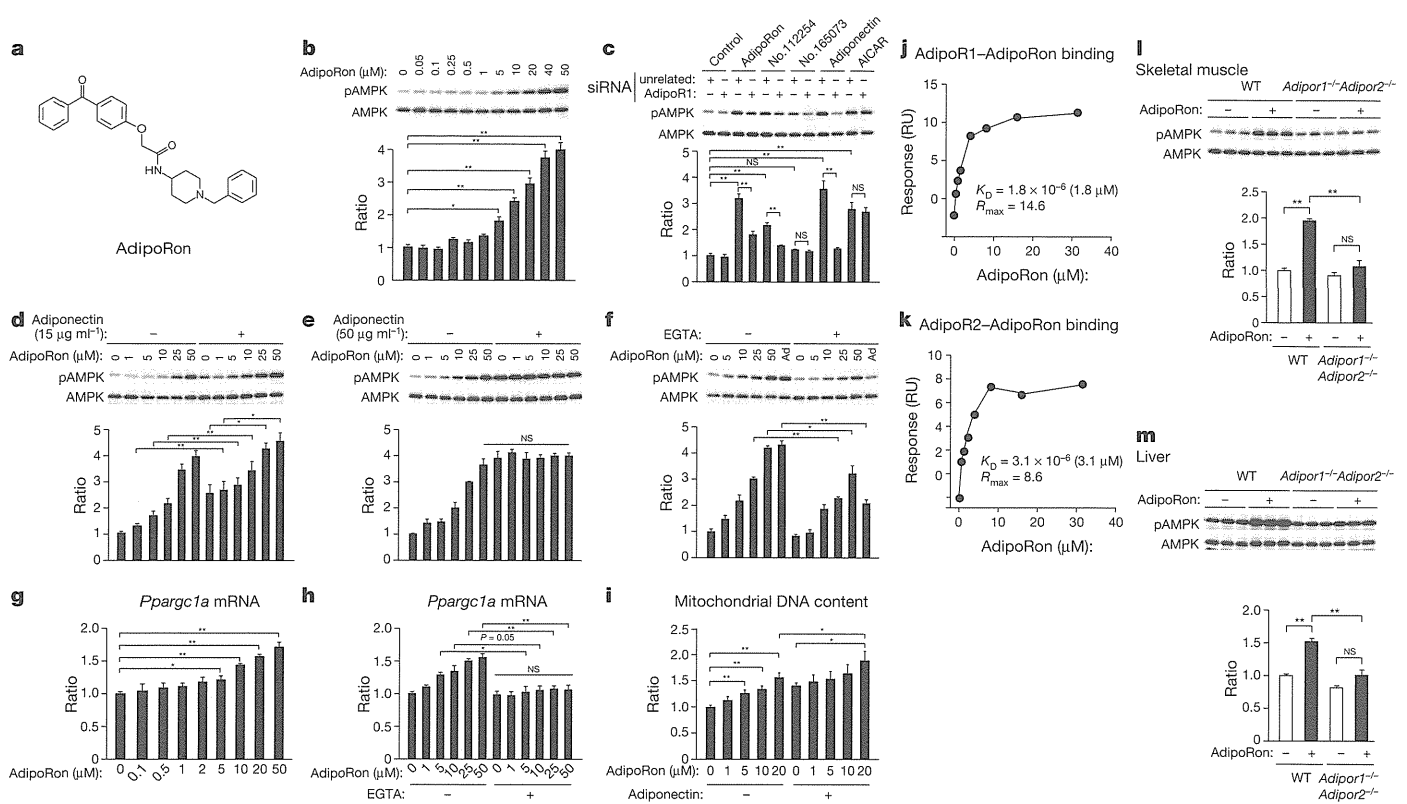


Figure 1 | Small-molecule AdipoR agonist AdipoRon binds to both AdipoR1 and AdipoR2, and increases AMPK activation, PGC-1 α expression and mitochondrial biogenesis in C2C12 myotubes. **a**, Chemical structure of AdipoRon. **b–i**, Phosphorylation and amount of AMPK (**b–f**, **l**, **m**), *Pparg1a* mRNA levels (**g**, **h**), and mitochondrial content as assessed by mitochondrial DNA copy number (**i**), in C2C12 myotubes after myogenic differentiation (**b–i**), in skeletal muscle (**l**) or in liver (**m**) from wild-type (WT) or *AdipoR1*^{-/-} *AdipoR2*^{-/-} double-knockout mice, treated with indicated concentrations of AdipoRon (**b**, **d–i**) or adiponectin (**d**, 15 $\mu\text{g ml}^{-1}$; **e**, 50 $\mu\text{g ml}^{-1}$; **i**, 10 $\mu\text{g ml}^{-1}$), for 5 min (**b**, **d–f**), 1.5 h (**g**, **h**) and 48 h (**i**), with or

without EGTA (**f**, **h**), 25 μM AdipoRon, compound 112254 and 165073, 30 $\mu\text{g ml}^{-1}$ adiponectin for 5 min or 1 mM AICAR for 1 h and transfected with or without the indicated siRNA duplex (**c**), or AdipoRon (**l**, **m**). **j**, **k**, Surface plasmon resonance measuring AdipoRon binding to AdipoR1 and AdipoR2. AdipoR1 and AdipoR2 were immobilized onto a sensor chip SA. Binding analyses were performed using a range of AdipoRon concentrations (0.49–31.25 μM). All values are presented as mean \pm s.e.m. **b**, **c**, **e–I**, $n = 4$ each; **d**, **l**, **m**, $n = 3$ each; * $P < 0.05$ and ** $P < 0.01$ compared to control or unrelated siRNA or as indicated. NS, not significant.

AMPK via AdipoR1, albeit less potently, and compound 165073 (a non-hit) failed to increase phosphorylation of AMPK (Fig. 1c).

In the presence or absence of the submaximal concentration of adiponectin (15 $\mu\text{g ml}^{-1}$), AdipoRon increased AMPK phosphorylation in a dose-dependent manner (Fig. 1d), whereas AdipoRon did not increase nor decrease AMPK phosphorylation in the presence of the maximal concentration of adiponectin (50 $\mu\text{g ml}^{-1}$) (Fig. 1e). These data suggested that AdipoRon replenished AMPK phosphorylation stimulated by adiponectin.

EGTA partially suppressed the AdipoRon-induced increase in AMPK phosphorylation in C2C12 myotubes (Fig. 1f), indicating that extracellular free Ca^{2+} is required for full AMPK phosphorylation stimulated with AdipoRon, like adiponectin²¹. Moreover, AdipoRon increased PGC-1 α (*Pparg1a*) expression (Fig. 1g, h) and mitochondrial DNA content (Fig. 1i) in a dose-dependent manner. Furthermore, EGTA effectively and almost completely abolished increased *Pparg1a* expression stimulated with AdipoRon in C2C12 myotubes (Fig. 1h), consistent with the report that increased PGC-1 α expression mediated by adiponectin is dependent on Ca^{2+} signalling²¹.

By using surface plasmon resonance, AdipoRon bound to both AdipoR1 and AdipoR2 (dissociation constant (K_D) of 1.8 and 3.1 μM ; R_{max} of 14.6 and 8.6 resonance units (RU), respectively) in a saturable manner (Fig. 1j, k). We also performed radioactive binding and Scatchard analysis and verified the specific binding of AdipoRon to AdipoR1 and AdipoR2 (Extended Data Fig. 4).

Intravenous injection of AdipoRon (50 mg kg^{-1} body weight) significantly induced phosphorylation of AMPK in skeletal muscle and liver

of wild-type mice but not *AdipoR1*^{-/-} *AdipoR2*^{-/-} double-knockout mice (Fig. 1l, m), indicating that AdipoRon could activate AMPK in skeletal muscle and liver via AdipoR1 and AdipoR2.

AdipoRon ameliorates diabetes via AdipoR

To clarify whether orally administered small-molecule AdipoR agonist AdipoRon would exhibit a pharmacokinetic profile suitable for *in vivo* evaluation in the mouse, we measured plasma concentrations of AdipoRon in C57BL/6 wild-type mice after oral administration of 50 mg kg^{-1} of AdipoRon, and found that the maximal concentration (C_{max}) of AdipoRon was 11.8 μM (Fig. 2a and Extended Data Fig. 5a).

To test the therapeutic potential of a small-molecule AdipoR agonist to treat insulin resistance and diabetes, the effects of orally administered AdipoRon were examined in high-fat-diet-induced obese mice. Oral administration of AdipoRon (50 mg kg^{-1} body weight) for 10 days did not significantly affect body weight (Fig. 2b) nor food intake (Fig. 2c) in mice on a high-fat diet, but it did significantly reduce fasting plasma glucose and insulin levels as well as glucose and insulin responses during oral glucose tolerance tests in wild-type mice treated with AdipoRon (Fig. 2d and Extended Data Fig. 5b, c). The decrease in glucose levels in the face of reduced plasma insulin levels indicates improved insulin sensitivity (Fig. 2d, f and Extended Data Fig. 5d, e). Notably, treatment of *AdipoR1*^{-/-} *AdipoR2*^{-/-} double-knockout mice with AdipoRon failed to ameliorate high-fat-diet-induced hyperglycaemia and hyperinsulinaemia (Fig. 2e, f and Extended Data Fig. 5f–i).

The glucose-lowering effect of exogenous insulin was also greater in AdipoRon-treated wild-type mice than in vehicle-treated control

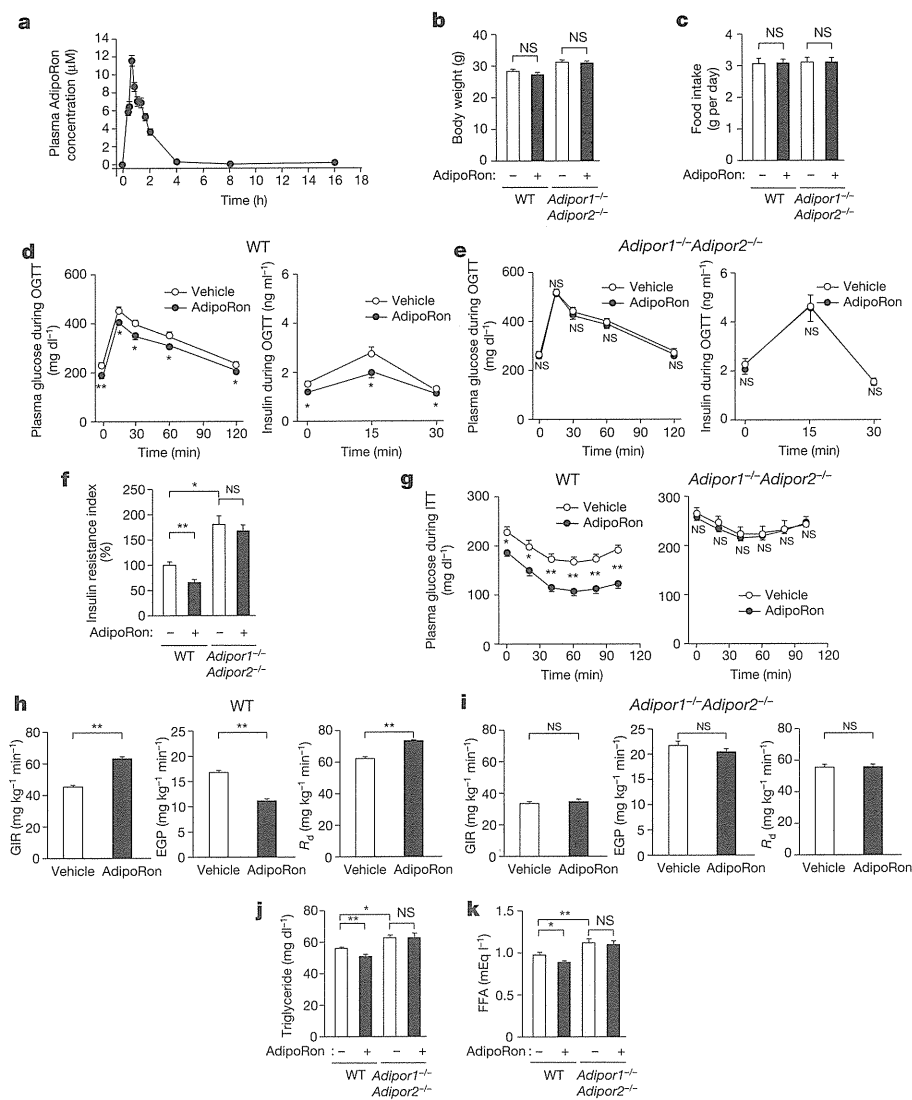


Figure 2 | AdipoRon improved insulin resistance, glucose intolerance and dyslipidaemia via AdipoR. **a–g**, Plasma AdipoRon concentrations (**a**), body weight (**b**), food intake (**c**), plasma glucose (**d, e, g**), plasma insulin (**d, e**) and insulin resistance index (**f**) during oral glucose tolerance test (OGTT) (1.0 g glucose per kg body weight) (**d, e**) or during insulin tolerance test (ITT) (0.5 U insulin per kg body weight) (**g**) in wild-type (WT) and *AdipoR1*^{-/-} *AdipoR2*^{-/-} double-knockout mice, treated with or without AdipoRon (50 mg per kg body weight). **h, i**, Glucose infusion rate (GIR), endogenous glucose production (EGP) and rates of glucose disposal (*R_d*) during hyperinsulinaemic euglycaemic clamp study in wild-type and *AdipoR1*^{-/-} *AdipoR2*^{-/-} double-knockout mice, treated with or without AdipoRon (50 mg per kg body weight). **j, k**, Plasma triglyceride (**j**) and free fatty acid (FFA) (**k**) in wild-type and *AdipoR1*^{-/-} *AdipoR2*^{-/-} double-knockout mice, treated with or without AdipoRon (50 mg per kg body weight). All values are presented as mean ± s.e.m. **a**, *n* = 12–32; **b–g, j, k**, *n* = 10 each; **h, i**, *n* = 5 each; **P* < 0.05 and ***P* < 0.01 compared to control or as indicated. NS, not significant.

wild-type mice (Fig. 2g, left, and Extended Data Fig. 5j, k), which was not observed in *AdipoR1*^{-/-} *AdipoR2*^{-/-} double-knockout mice (Fig. 2g, right, and Extended Data Fig. 5l, m).

We examined whether a similar chemical analogue of AdipoRon that could activate AMPK via AdipoR would have an antidiabetic effect. Consistent with this, we observed that another similar chemical analogue of AdipoRon, compound 112254 (Extended Data Fig. 6a), could activate AMPK (Fig. 1c) and at the same time ameliorate both glucose intolerance and insulin resistance (Extended Data Fig. 6c–f). Conversely, we observed that another compound, 165073 (Extended Data Fig. 6b), could not activate AMPK (Fig. 1c), ameliorate glucose intolerance, nor ameliorate insulin resistance (Extended Data Fig. 6g–j).

We performed hyperinsulinaemic euglycaemic clamps in mice on a high-fat diet after 10 days of treatment. The glucose infusion rate was significantly increased (Fig. 2h, left), the endogenous glucose production was significantly suppressed (Fig. 2h, middle), and the glucose disposal rate was significantly increased (Fig. 2h, right) in AdipoRon-treated wild-type mice. None of these parameters was improved on AdipoRon treatment in *AdipoR1*^{-/-} *AdipoR2*^{-/-} double-knockout mice (Fig. 2i).

We next examined the effects of AdipoRon on lipid metabolism. Treatment with AdipoRon for 10 days reduced plasma concentrations of triglycerides and free fatty acid (FFA) in wild-type mice fed a high-fat diet (Fig. 2j, k), an effect that was not observed in *AdipoR1*^{-/-} *AdipoR2*^{-/-} double-knockout mice (Fig. 2j, k).

AdipoRon activates AdipoR1-AMPK-PGC-1α pathways

In skeletal muscle of wild-type mice, AdipoRon increased the expression of genes involved in mitochondrial biogenesis such as *Ppargc1a* and oestrogen-related receptor-α (*Esrra*)²⁹, mitochondrial DNA replication/translation such as mitochondrial transcription factor A (*Tfam*), and oxidative phosphorylation such as cytochrome *c* oxidase subunit II (*mt-Co2*) (Fig. 3a). AdipoRon also increased mitochondrial DNA content in the skeletal muscle of wild-type mice (Fig. 3b). These effects were completely obliterated in *AdipoR1*^{-/-} *AdipoR2*^{-/-} double-knockout mice (Fig. 3a, b).

AdipoRon increased the levels of oxidative, high endurance type I fibre³⁰ marker troponin I (slow) (*Tnni1*) in the skeletal muscle of wild-type mice (Fig. 3a) but not in *AdipoR1*^{-/-} *AdipoR2*^{-/-} double-knockout mice (Fig. 3a). We challenged mice fed a high-fat diet with involuntary physical exercise by treadmill running and then assessed muscle endurance. AdipoRon significantly increased exercise endurance in wild-type mice, but not in *AdipoR1*^{-/-} *AdipoR2*^{-/-} double-knockout mice (Fig. 3c) fed a high-fat diet.

We next examined the expression of metabolic genes and found that AdipoRon significantly increased the expression of genes involved in fatty-acid oxidation such as medium-chain acyl-CoA dehydrogenase (*Acadm*) (Fig. 3a), which was associated with decreased triglyceride content³¹ (Extended Data Fig. 7a), in the skeletal muscle of wild-type mice but not of *AdipoR1*^{-/-} *AdipoR2*^{-/-} double-knockout mice fed a high-fat diet.

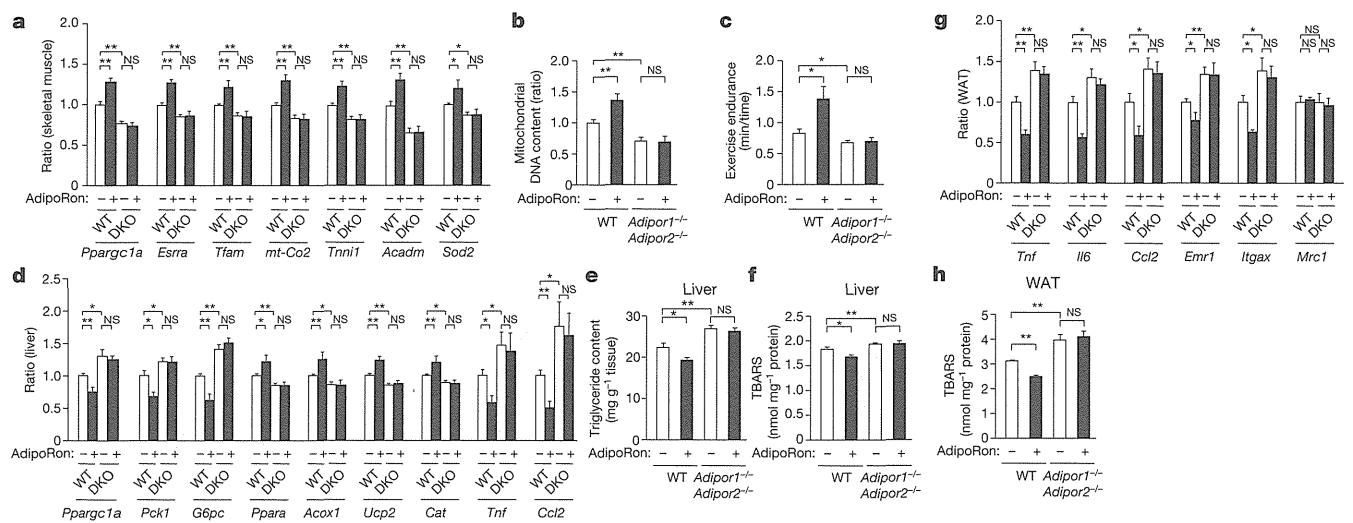


Figure 3 | AdipoRon increased mitochondria biogenesis in muscle, reduced tissue triglyceride content in liver and decreased oxidative stress and inflammation in liver and WAT. a–h, *Ppargc1a*, *Esrra*, *Tfam*, *mt-Co2*, *Tnni1*, *Acadm* and *Sod2* mRNA levels (a), mitochondrial content as assessed by mitochondrial DNA copy number (b) in skeletal muscle, exercise endurance (c), *Ppargc1a*, *Pck1*, *G6pc*, *Ppara*, *Acox1*, *Ucp2*, *Cat*, *Tnf* and *Ccl2* mRNA levels

(d), tissue triglyceride content (e), TBARS (f) in liver and *Tnf*, *Il6*, *Ccl2*, *Emr1*, *Itgax* and *Mrc1* mRNA levels (g) and TBARS (h) in WAT, from wild-type and *Adipor1*^{-/-} *Adipor2*^{-/-} double-knockout (DKO) mice treated with or without AdipoRon (50 mg per kg body weight). All values are presented as mean ± s.e.m. a, b, d–h, *n* = 10 each; c, *n* = 5 each; **P* < 0.05 and ***P* < 0.01 compared to control or as indicated. NS, not significant.

AdipoRon significantly increased the expression levels for oxidative stress-detoxifying genes such as manganese superoxide dismutase (*Sod2*) (Fig. 3a), and decreased oxidative stress markers³² such as thiobarbituric acid reactive substance (TBARS) (Extended Data Fig. 7b), in the skeletal muscle of wild-type mice but not of *Adipor1*^{-/-} *Adipor2*^{-/-} double-knockout mice fed a high-fat diet.

AdipoRon also activates AdipoR2–PPAR- α pathways

We examined whether AdipoRon could activate AdipoR1 and AdipoR2 pathways in the liver. The activation of AdipoR1–AMPK pathway in the liver has been reported to reduce the expression of genes involved in hepatic gluconeogenesis such as *Ppargc1a*, phosphoenolpyruvate carboxykinase 1 (*Pck1*)^{20,33} and glucose-6-phosphatase (*G6pc*). As predicted by these earlier studies, we found that AdipoRon significantly decreased the expression of *Ppargc1a*, *Pck1* and *G6pc* in the liver of wild-type (Fig. 3d) but not of *Adipor1*^{-/-} *Adipor2*^{-/-} double-knockout mice (Fig. 3d) fed a high-fat diet.

Activation of AdipoR2 can increase PPAR- α levels and activate PPAR- α pathways, leading to increased fatty-acid oxidation and reduction of oxidative stress²⁰. AdipoRon increased the expression levels of the gene encoding PPAR- α itself (*Ppara*) and its target genes¹⁶, including genes involved in fatty-acid combustion such as acyl-CoA oxidase (*Acox1*), genes involved in energy dissipation such as uncoupling protein 2 (*Ucp2*), and genes encoding oxidative stress detoxifying enzymes such as catalase (*Cat*) in the liver of wild-type (Fig. 3d) but not of *Adipor1*^{-/-} *Adipor2*^{-/-} double-knockout mice (Fig. 3d) fed a high-fat diet. AdipoRon significantly reduced triglyceride content (Fig. 3e) and oxidative stress³², as measured by TBARS (Fig. 3f), in the liver of wild-type mice but not of *Adipor1*^{-/-} *Adipor2*^{-/-} double-knockout mice (Fig. 3e, f) fed a high-fat diet.

Notably, orally administered AdipoRon reduced the expression levels of the genes encoding pro-inflammatory cytokines such as TNF- α (*Tnf*)³⁴ and MCP-1 (*Ccl2*) in the liver of wild-type mice (Fig. 3d) but not of *Adipor1*^{-/-} *Adipor2*^{-/-} double-knockout mice (Fig. 3d) fed a high-fat diet.

AdipoRon decreases inflammation

AdipoRon reduced the expression levels of genes encoding pro-inflammatory cytokines^{35–37} such as *Tnf*, IL-6 (*Il6*) and *Ccl2* in the white

adipose tissue (WAT) of wild-type mice but not of *Adipor1*^{-/-} *Adipor2*^{-/-} double-knockout mice fed a high-fat diet (Fig. 3g). Notably, AdipoRon reduced TBARS (Fig. 3h) and reduced levels of macrophage markers such as F4/80 (*Emr1*), and especially the levels of markers for classically activated M1 macrophages such as CD11c (*Itgax*)³⁸—but not the levels of markers for the alternatively activated M2 macrophages such as CD206 (*Mrc1*)—in the WAT of wild-type mice fed a high-fat diet (Fig. 3g), whereas these changes were not observed in *Adipor1*^{-/-} *Adipor2*^{-/-} double-knockout mice (Fig. 3g, h).

AdipoRon ameliorates diabetes in *db/db* mice

We next studied the effects of AdipoRon (50 mg kg⁻¹ body weight) in a genetically obese rodent model (*Lepr*^{-/-} (also known as *db/db*) mice); *db/db* mice fed a normal chow diet exhibit decreased plasma adiponectin concentrations^{6,10}. As was expected¹³, intraperitoneal injection of adiponectin into *db/db* mice reduced plasma glucose levels (Fig. 4a, left and right panels). Interestingly, orally administered AdipoRon also significantly reduced plasma glucose levels as quickly and potently as did intraperitoneal adiponectin injection in *db/db* mice (Fig. 4a, middle and right panels).

Without affecting body weight, food intake, liver weight and WAT weight (Fig. 4b–e), orally administered AdipoRon for 2 weeks significantly ameliorated glucose intolerance, insulin resistance and dyslipidaemia in *db/db* mice fed a normal chow diet (Fig. 4f–i).

In the skeletal muscle of *db/db* mice fed a normal chow diet, AdipoRon significantly increased the expression levels of genes involved in mitochondrial biogenesis functions and DNA content (Fig. 5a, b), and also *Acadm* and *Sod2* (Fig. 5a), which were associated with decreased triglyceride content and TBARS (Fig. 5c, d), respectively. In the liver, AdipoRon significantly decreased the expression of *Ppargc1a*, *Pck1* and *G6pc* (Fig. 5e), increased the expression of *Ppara* and its target genes (Fig. 5e). Therefore, Adipron significantly reduced triglyceride content (Fig. 5f), oxidative stress (Fig. 5g) and reduced the expression levels of genes encoding pro-inflammatory cytokines (Fig. 5e). In the WAT, AdipoRon reduced the expression levels of genes encoding pro-inflammatory cytokines and macrophage markers, especially the levels of markers for classically activated M1 macrophages, but not the levels of markers for the alternatively activated M2 macrophages (Fig. 5h).

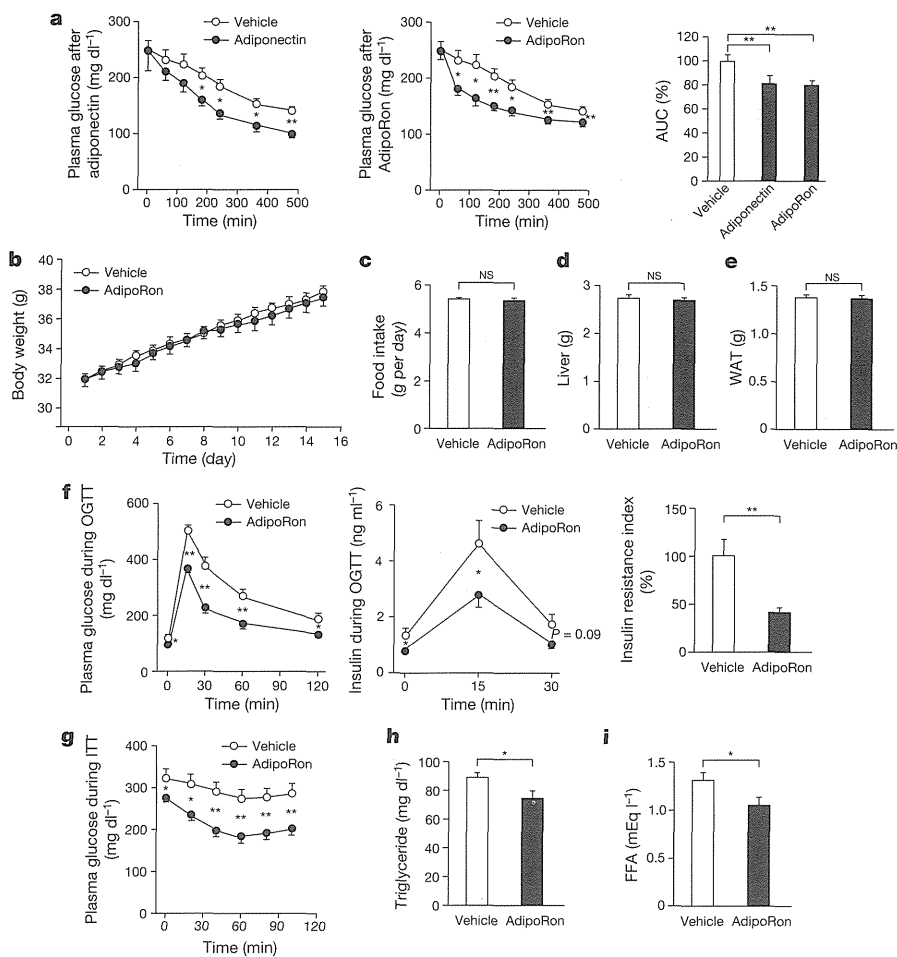


Figure 4 | AdipoRon ameliorated insulin resistance, diabetes and dyslipidaemia in *db/db* mice. **a**, Plasma glucose levels after intraperitoneal injection of adiponectin (30 μ g per 10 g body weight) (left) or after oral administration of AdipoRon (50 mg per kg body weight) (middle). The area under the curve (AUC) of left and middle panels is shown on the right. **b–i**, Body weight (**b**), food intake (**c**), liver weight (**d**), WAT weight (**e**), plasma glucose (**f**, left, **g**), plasma insulin (**f**, middle) and insulin resistance index (**f**, right) during oral glucose tolerance test (OGTT) (1.0 g glucose per kg body weight) (**f**) or during insulin tolerance test (ITT) (0.75 U insulin per kg body weight) (**g**), plasma triglyceride (**h**) and free fatty acid (FFA) (**i**) in *db/db* mice under normal chow conditions, treated with or without AdipoRon (50 mg per kg body weight). All values are presented as mean \pm s.e.m. **a**, $n = 6-7$; **b–i**, $n = 10$ each from 2–3 independent experiments, * $P < 0.05$ and ** $P < 0.01$ compared to control or as indicated. NS, not significant.

AdipoRon prolonged the shortened lifespan

Notably, *Adipor1*^{-/-}*Adipor2*^{-/-} double-knockout mice showed a shortened lifespan as compared with wild-type mice under both normal chow diet and high-fat diet conditions (Fig. 6a, b). Because a high-fat diet has been reported to shorten lifespan³⁹, we examined whether orally administered AdipoR agonists could prolong the shortened lifespan on a high-fat diet. Lifespan of *db/db* mice on a high-fat diet was markedly shortened as compared with that on a normal chow diet. Surprisingly, AdipoRon significantly rescued the shortened lifespan of *db/db* mice on a high-fat diet (Fig. 6c).

The decreased effects of adiponectin in obesity have been reported to have causal roles in the development of obesity-related diseases such as diabetes⁴⁰ and cardiovascular diseases⁴¹. There are two strategies to reverse reduced adiponectin effects. One is to increase the levels of adiponectin itself, such as through the injection of adiponectin. However, there are many difficulties associated with adiponectin injection, such as very high plasma concentrations of adiponectin and high-molecular-weight adiponectin multimers as highest activity form⁴².

An alternative strategy is to activate adiponectin receptors. Both AdipoR1 and AdipoR2 have roles in the regulation of glucose and lipid metabolism, inflammation, and oxidative stress *in vivo*²⁰. Therefore, the development of orally active small-molecule agonists for both AdipoR1 and AdipoR2 has long been sought. Here, we have identified and characterized an orally active synthetic small molecule that binds to and activates AdipoR1 and AdipoR2. So far, the top four hits obtained through the screening campaign have common structural motifs (Extended Data Fig. 8) (see additional results and discussion in Supplementary Information).

One of these small molecules, AdipoRon, binds to both AdipoR1 and AdipoR2 *in vitro* (K_d 1.8 and 3.1 μ M; R_{max} 14.6 and 8.6 RU, respectively), activates AMPK, and increases PGC-1 α levels and mitochondrial DNA content in myotubes (Fig. 1). When AdipoRon was administered orally to mice (50 mg per kg body weight), it was confirmed that the concentrations of AdipoRon in plasma (C_{max} of 11.8 μ M) reached levels greater than the K_d values (AdipoR1, 1.8 μ M; AdipoR2, 3.1 μ M) (Fig. 2a). After the concentration reached the maximum as shown in Fig. 2a, the effect reached the maximum (Extended Data Fig. 5n), and the effect lasted for at least 8 h. Orally administered AdipoRon ameliorated insulin resistance, glucose intolerance and dyslipidaemia in mice fed a high-fat diet (Fig. 2d–k). Notably, these beneficial effects were completely obliterated in *Adipor1*^{-/-}*Adipor2*^{-/-} double-knockout mice (Fig. 2d–k) but partially preserved in *Adipor1*^{-/-} or *Adipor2*^{-/-} single-knockout mice (Extended Data Fig. 7c–g), indicating that AdipoRon works through both AdipoR1 and AdipoR2 *in vivo*.

Adiponectin ameliorated insulin resistance and glucose intolerance via multiple mechanisms including activation of AMPK, decreased oxidative stress, decreased tissue triglyceride content and suppression of inflammation^{13,14}. AdipoRon exerted multiple effects very similar to those of adiponectin described above *in vivo*, and ameliorated insulin resistance and glucose intolerance via AdipoR1 and AdipoR2 in obese diabetic mice on a high-fat diet (Fig. 3).

In this study, we show that in skeletal muscle of obese diabetic mice such as wild-type mice on a high-fat diet (Fig. 3) and *db/db* mice (Figs 4 and 5), AdipoR1 and AdipoR2 agonists such as AdipoRon increase mitochondrial biogenesis, which was associated with increased

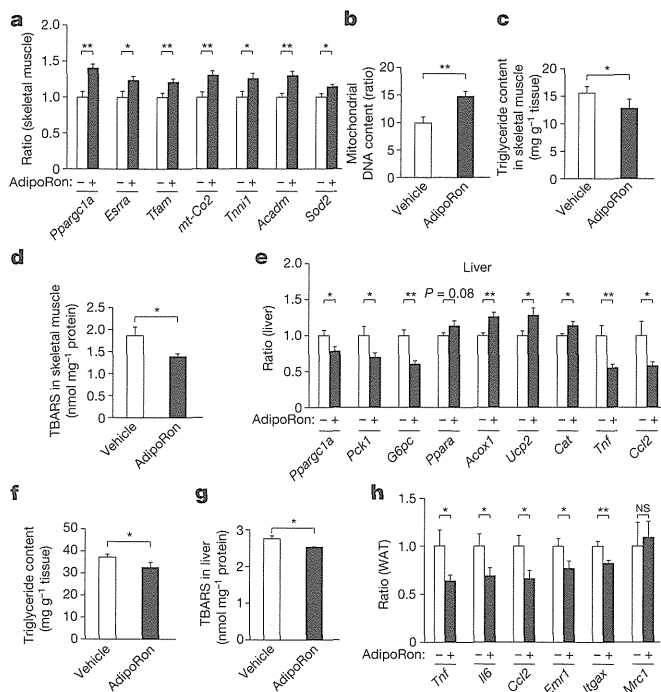


Figure 5 | AdipoRon increased mitochondria biogenesis in muscle, reduced tissue triglyceride content and oxidative stress in muscle and liver, and decreased inflammation in liver and WAT of *db/db* mice. a–h, *Pparg1a*, *Esrra*, *Tfam*, *mt-Co2*, *Tnni1*, *Acadm* and *Sod2* mRNA levels (a), and mitochondrial content as assessed by mitochondrial DNA copy number (b), tissue triglyceride content (c) and TBARS (d) in skeletal muscle, *Pparg1a*, *Pck1*, *G6pc*, *Ppara*, *Acox1*, *Ucp2*, *Cat*, *Tnf* and *Ccl2* mRNA levels (e), tissue triglyceride content (f) and TBARS (g) in liver, and *Tnf*, *Il6*, *Ccl2*, *Emr1*, *Itgax* and *Mrc1* mRNA levels (h) in WAT from *db/db* mice on a normal chow diet, treated with or without AdipoRon (50 mg per kg body weight). All values are presented as mean ± s.e.m. *n* = 10, **P* < 0.05 and ***P* < 0.01 compared to control or as indicated. NS, not significant.

exercise endurance, and at the same time increase expression levels of genes involved in fatty-acid combustion, oxidative phosphorylation and reduction of oxidative stress (Figs 3, 5 and 6d). In liver, AdipoRon suppresses the expression of genes involved in gluconeogenesis, increases expression of PPAR-α target genes involved in fatty-acid combustion, and reduces oxidative stress (Figs 3, 5 and 6d). In WAT, AdipoRon reduces oxidative stress and pro-inflammatory cytokines, and the accumulation of M1 macrophages (Figs 3, 5 and 6d). Importantly, these effects resulted in reduced tissue triglyceride content in liver and muscle, and oxidative stress in liver, muscle and WAT, and decreased inflammation in liver and WAT (Figs 3–5 and 6d). These alterations collectively result in increased insulin sensitivity and glucose tolerance (Fig. 6d).

Therefore, we could expect AdipoRon to exert most, if not all, of the effects exerted by adiponectin, such as increased insulin sensitivity and glucose tolerance, as well as suppression of cardiovascular diseases and cancer, as previously reported^{17,41,43}. Indeed, AdipoRon did prolong the shortened lifespan of obese diabetic mice (Fig. 6a–d).

Taken together, our findings show that the orally active small-molecule AdipoR agonist AdipoRon shifts the physiology of mice fed excess calorie towards that of mice fed a standard diet, modulates known longevity pathways, and improves health and prolongs lifespan. This study provides evidence that an orally available synthetic small-molecule AdipoR agonist at doses achievable *in vivo* can safely reduce many of the unhealthy and undesirable consequences of excess calorie intake and sedentary lifestyle, with an overall improvement in health and even lifespan, much like calorie restriction and exercise. Because virtually all current therapeutic modalities of type 2 diabetes require stringent adherence to diet and exercise and are associated with adverse effects such as hypoglycaemia and weight gain, AdipoRon provides a novel pre-emptive medicine and treatment modality. Orally active AdipoR agonists are a promising novel therapeutic approach for treating obesity-related disorders such as type 2 diabetes.

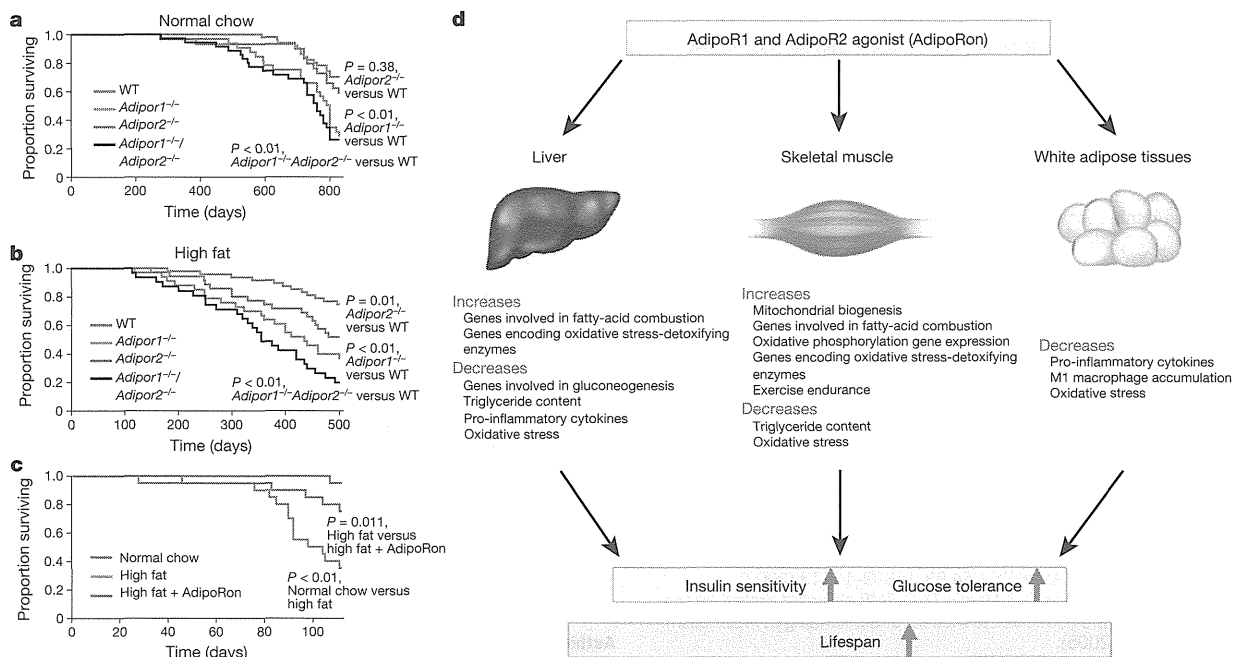


Figure 6 | AdipoRon increased insulin sensitivity and glucose tolerance, and at the same time contributed to longevity of obese diabetic mice. a–c, Kaplan–Meier survival curves for wild-type, *Adipor1*^{-/-}, *Adipor2*^{-/-} and *Adipor1*^{-/-}*Adipor2*^{-/-} knockout mice on a normal chow diet (a) (*n* = 50, 32, 29 and 35, respectively) or high-fat diet (b) (*n* = 47, 33, 35 and 31, respectively),

or for *db/db* mice treated with or without AdipoRon (30 mg per kg body weight) on a normal chow or high-fat diet (*n* = 20 each) (c). *P* values were derived from log-rank calculations. d, Scheme illustrating the mechanisms by which AdipoR1 and AdipoR2 agonist increases insulin sensitivity and glucose tolerance, and at the same time lifespan. (See also main text.)

METHODS SUMMARY

Mice. Mice were 6–10 weeks of age at the time of the experiment. The animal care and use procedures were approved by the Animal Care Committee of the University of Tokyo (see additional Methods in Supplementary Information).

Studies with C2C12 cells. Induction of myogenic differentiation was carried out according to a method described previously²¹. By day 5, the cells had differentiated into multinucleated contracting myotubes. C2C12 myotubes were used after myogenic differentiation in all experiments.

Survival. The wild-type, *Adipor1*^{-/-}, *Adipor2*^{-/-}, *Adipor1*^{-/-} *Adipor2*^{-/-} knockout mice and the *db/db* mice were maintained with food and water ad libitum. In these experiments, we used standard chow diet (CE-2, CLEA Japan Inc.) or high-fat diet 32 (CLEA Japan Inc.)²⁰. For the experiment shown in Fig. 6a, b, wild-type (*n* = 50), *Adipor1*^{-/-} (*n* = 32), *Adipor2*^{-/-} (*n* = 29) and *Adipor1*^{-/-} *Adipor2*^{-/-} (*n* = 35) knockout mice fed a normal chow diet were used. For the experiment shown in Fig. 6b, wild-type (*n* = 47), *Adipor1*^{-/-} (*n* = 33), *Adipor2*^{-/-} (*n* = 35) and *Adipor1*^{-/-} *Adipor2*^{-/-} (*n* = 31) knockout mice on a high-fat diet were used. For the experiment shown in Fig. 6c, the *db/db* mice were randomly divided into three groups: a normal chow group (normal chow, *n* = 20), high-fat group (high fat, *n* = 20) and high-fat plus AdipoRon group (high fat + AdipoRon, *n* = 20), which were treated with AdipoRon at a daily dose of 30 mg kg⁻¹ body weight. The survival rate was recorded daily. Survival curves were plotted using the Kaplan–Meier method.

Statistical analysis. Results are expressed as mean ± s.e.m. Differences between two groups were assessed using unpaired two-tailed *t*-tests. Data involving more than two groups were assessed by analysis of variance (ANOVA).

Online Content Any additional Methods, Extended Data display items and Source Data are available in the online version of the paper; references unique to these sections appear only in the online paper.

Received 6 June 2012; accepted 10 September 2013.

Published online 30 October 2013.

- Gesta, S., Tseng, Y. H. & Kahn, C. R. Developmental origin of fat: tracking obesity to its source. *Cell* **131**, 242–256 (2007).
- Olefsky, J. M. & Glass, C. K. Macrophages, inflammation, and insulin resistance. *Annu. Rev. Physiol.* **72**, 219–246 (2010).
- Osler, M. E. & Zierath, J. R. Adenosine 5'-monophosphate-activated protein kinase regulation of fatty acid oxidation in skeletal muscle. *Endocrinology* **149**, 935–941 (2008).
- LeRoith, D. & Accili, D. Mechanisms of disease: using genetically altered mice to study concepts of type 2 diabetes. *Nature Clin. Pract. Endocrinol. Metab.* **4**, 164–172 (2008).
- Scherer, P. E., Williams, S., Fogliano, M., Baldini, G. & Lodish, H. F. A novel serum protein similar to C1q, produced exclusively in adipocytes. *J. Biol. Chem.* **270**, 26746–26749 (1995).
- Hu, E., Liang, P. & Spiegelman, B. M. AdipoQ is a novel adipose-specific gene dysregulated in obesity. *J. Biol. Chem.* **271**, 10697–10703 (1996).
- Maeda, K. *et al.* cDNA cloning and expression of a novel adipose specific collagen-like factor, apM1 (AdiPose most abundant gene transcript 1). *Biochem. Biophys. Res. Commun.* **221**, 286–289 (1996).
- Nakano, Y., Tobe, T., Choi-Miura, N. H., Mazda, T. & Tomita, M. Isolation and characterization of GBP28, a novel gelatin-binding protein purified from human plasma. *J. Biochem.* **120**, 803–812 (1996).
- Hotta, K. *et al.* Plasma concentrations of a novel, adipose-specific protein, adiponectin, in type 2 diabetic patients. *Arterioscler. Thromb. Vasc. Biol.* **20**, 1595–1599 (2000).
- Yamauchi, T. *et al.* The fat-derived hormone adiponectin reverses insulin resistance associated with both lipodystrophy and obesity. *Nature Med.* **7**, 941–946 (2001).
- Berg, A. H., Combs, T. P., Du, X., Brownlee, M. & Scherer, P. E. The adipocyte-secreted protein Acrp30 enhances hepatic insulin action. *Nature Med.* **7**, 947–953 (2001).
- Fruebis, J. *et al.* Proteolytic cleavage product of 30-kDa adipocyte complement-related protein increases fatty acid oxidation in muscle and causes weight loss in mice. *Proc. Natl Acad. Sci. USA* **98**, 2005–2010 (2001).
- Yamauchi, T. *et al.* Adiponectin stimulates glucose utilization and fatty-acid oxidation by activating AMP-activated protein kinase. *Nature Med.* **8**, 1288–1295 (2002).
- Tomas, E. *et al.* Enhanced muscle fat oxidation and glucose transport by ACRP30 globular domain: acetyl-CoA carboxylase inhibition and AMP-activated protein kinase activation. *Proc. Natl Acad. Sci. USA* **99**, 16309–16313 (2002).
- Kahn, B. B., Alquier, T., Carling, D. & Hardie, D. G. AMP-activated protein kinase: ancient energy gauge provides clues to modern understanding of metabolism. *Cell Metab.* **1**, 15–25 (2005).
- Kersten, S., Desvergne, B. & Wahli, W. Roles of PPARs in health and disease. *Nature* **405**, 421–424 (2000).
- Yamauchi, T. *et al.* Globular adiponectin protected ob/ob mice from diabetes and apoE deficient mice from atherosclerosis. *J. Biol. Chem.* **278**, 2461–2468 (2003).

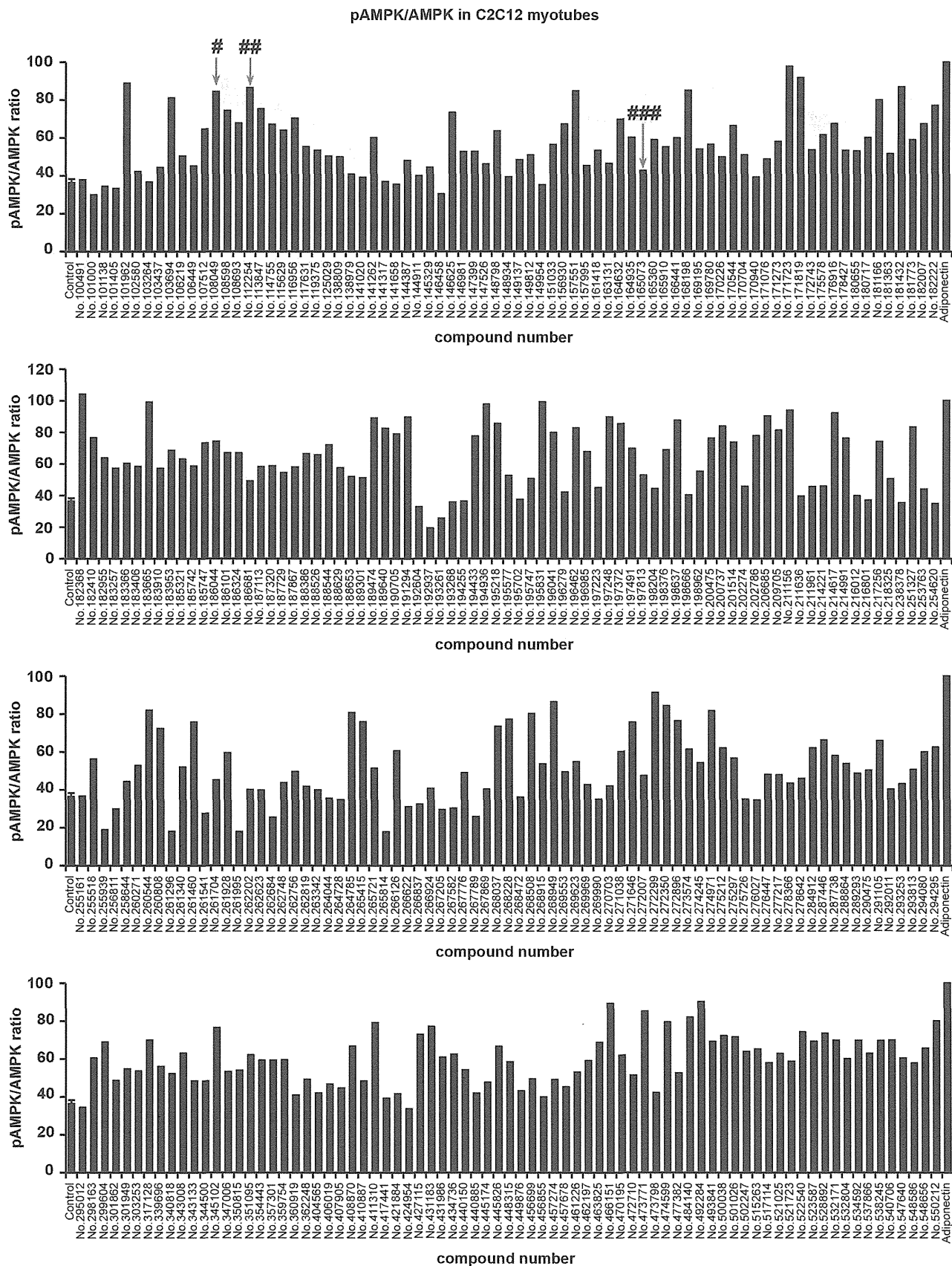
- Yamauchi, T. *et al.* Cloning of adiponectin receptors that mediate antidiabetic metabolic effects. *Nature* **423**, 762–769 (2003).
- Wess, J. G-protein-coupled receptors: molecular mechanisms involved in receptor activation and selectivity of G-protein recognition. *FASEB J.* **11**, 346–354 (1997).
- Yamauchi, T. *et al.* Targeted disruption of AdipoR1 and AdipoR2 causes abrogation of adiponectin binding and metabolic actions. *Nature Med.* **13**, 332–339 (2007).
- Iwabu, M. *et al.* Adiponectin and AdipoR1 regulate PGC-1 α and mitochondria by Ca²⁺ and AMPK/SIRT1. *Nature* **464**, 1313–1319 (2010).
- Richter, E. A. & Ruderman, N. B. AMPK and the biochemistry of exercise: implications for human health and disease. *Biochem. J.* **418**, 261–275 (2009).
- Wu, Z. *et al.* Mechanisms controlling mitochondrial biogenesis and respiration through the thermogenic coactivator PGC-1. *Cell* **98**, 115–124 (1999).
- Handschin, C. & Spiegelman, B. M. The role of exercise and PGC1 α in inflammation and chronic disease. *Nature* **454**, 463–469 (2008).
- Cantó, C. *et al.* AMPK regulates energy expenditure by modulating NAD⁺ metabolism and SIRT1 activity. *Nature* **458**, 1056–1060 (2009).
- Paffenbarger, R. S. Jr *et al.* The association of changes in physical-activity level and other lifestyle characteristics with mortality among men. *N. Engl. J. Med.* **328**, 538–545 (1993).
- Open Innovation Center for Drug Discovery. http://www.ocdd.u-tokyo.ac.jp/library_e.html (The University of Tokyo, 2012).
- Hawley, S. A. *et al.* Characterization of the AMP-activated protein kinase from rat liver and identification of threonine 172 as the major site at which it phosphorylates AMP-activated protein kinase. *J. Biol. Chem.* **271**, 27879–27887 (1996).
- Mootha, V. K. *et al.* *Erra* and *Gabpa/b* specify PGC-1 α -dependent oxidative phosphorylation gene expression that is altered in diabetic muscle. *Proc. Natl Acad. Sci. USA* **101**, 6570–6575 (2004).
- Berchtold, M. W. *et al.* Calcium ion in skeletal muscle: its crucial role for muscle function, plasticity, and disease. *Physiol. Rev.* **80**, 1215–1265 (2000).
- Shulman, G. I. Cellular mechanisms of insulin resistance. *J. Clin. Invest.* **106**, 171–176 (2000).
- Brownlee, M. Biochemistry and molecular cell biology of diabetic complications. *Nature* **414**, 813–820 (2001).
- Lochhead, P. A. *et al.* 5-aminoimidazole-4-carboxamide riboside mimics the effects of insulin on the expression of the 2 key gluconeogenic genes PEPCK and glucose-6-phosphatase. *Diabetes* **49**, 896–903 (2000).
- Hotamisligil, G. S., Shargill, N. S. & Spiegelman, B. M. Adipose expression of tumor necrosis factor- α : direct role in obesity-linked insulin resistance. *Science* **259**, 87–91 (1993).
- Wellen, K. E. & Hotamisligil, G. S. Inflammation, stress, and diabetes. *J. Clin. Invest.* **115**, 1111–1119 (2005).
- Weisberg, S. P. *et al.* Obesity is associated with macrophage accumulation in adipose tissue. *J. Clin. Invest.* **112**, 1796–1808 (2003).
- Xu, H. *et al.* Chronic inflammation in fat plays a crucial role in the development of obesity-related insulin resistance. *J. Clin. Invest.* **112**, 1821–1830 (2003).
- Lumeng, C. N., Bodzin, J. L. & Saltiel, A. R. Obesity induces a phenotypic switch in adipose tissue macrophage polarization. *J. Clin. Invest.* **117**, 175–184 (2007).
- Zhang, H. M. *et al.* Geldanamycin derivative ameliorates high fat diet-induced renal failure in diabetes. *PLoS ONE* **7**, e32746 (2012).
- Li, S., Shin, H. J., Ding, E. L. & van Dam, R. M. Adiponectin levels and risk of type 2 diabetes: a systematic review and meta-analysis. *J. Am. Med. Assoc.* **302**, 179–188 (2009).
- Pischon, T. *et al.* Plasma adiponectin levels and risk of myocardial infarction in men. *J. Am. Med. Assoc.* **291**, 1730–1737 (2004).
- Pajvani, U. B. *et al.* Complex distribution, not absolute amount of adiponectin, correlates with thiazolidinedione-mediated improvement in insulin sensitivity. *J. Biol. Chem.* **279**, 12152–12162 (2004).
- Luo, Z., Saha, A. K., Xiang, X. & Ruderman, N. B. AMPK, the metabolic syndrome and cancer. *Trends Pharmacol. Sci.* **26**, 69–76 (2005).

Supplementary Information is available in the online version of the paper.

Acknowledgements We thank N. Kubota, K. Hara, I. Takamoto, Y. Hada, T. Kobori, H. Urmematsu, S. Odawara, T. Aoyama, Y. Jing, S. Wei, K. Soeda and H. Waki for technical help and support; and K. Miyata, Y. Nishibaba, M. Yuasa and A. Hayashi for technical assistance and support. This work was supported by a Grant-in-aid for Scientific Research (S) (20229008, 25221307) (to T.K.), Grant-in-aid for Young Scientists (A) (23689048) (to M.I.), Targeted Proteins Research Program (to T.K.), the Global COE Research Program (to T.K.), Translational Systems Biology and Medicine Initiative (to T.K.) and Translational Research Network Program (to M.O.-I.) from the Ministry of Education, Culture, Sports, Science and Technology of Japan. Funding Program for Next Generation World-Leading Researchers (NEXT Program) (to T.Y.) from Cabinet Office, Government of Japan.

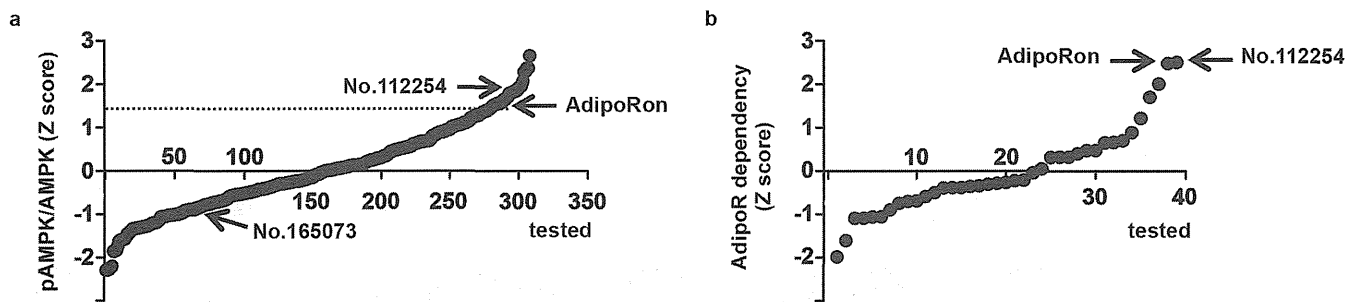
Author Contributions M.O.-I., M.I., T.Y., T.H., K.-i.-H., K.M., M.Y., H.T., T.K.-S., M.S., H.O., K.T. and A.T. performed experiments. T.K., T.Y., M.O.-I. and M.I. conceived the study. T.K., A.T., T.Y. and S.Y. supervised the study. T.Y., T.K., M.O.-I. and M.I. wrote the paper. All authors interpreted data.

Author Information Reprints and permissions information is available at www.nature.com/reprints. The authors declare no competing financial interests. Readers are welcome to comment on the online version of the paper. Correspondence and requests for materials should be addressed to T.K. (kadowaki-3im@h.u-tokyo.ac.jp) or T.Y. (tyamau-ky@umin.net).



Extended Data Figure 1 | Phosphorylation of AMPK in C2C12 myotubes. Phosphorylation of AMPK normalized to the amount of AMPK in C2C12

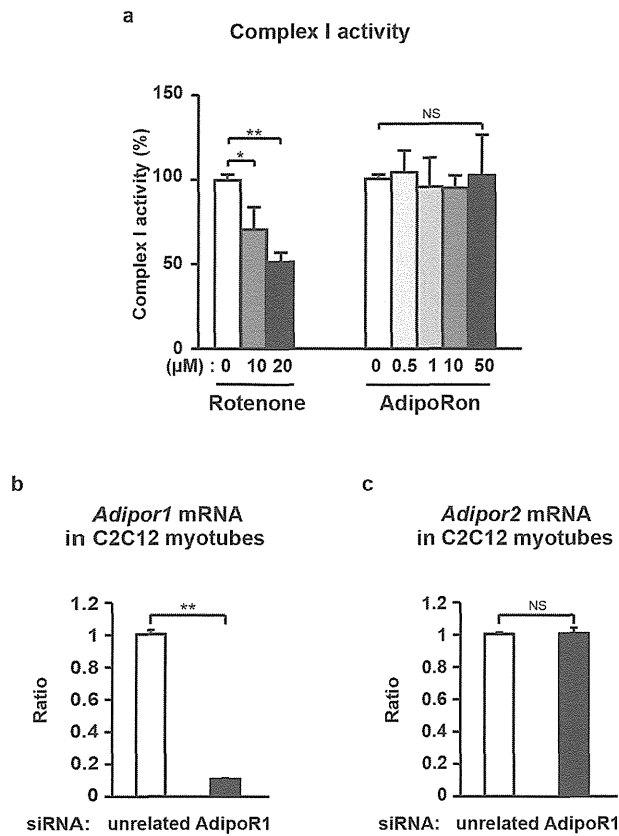
myotubes treated for 5 min with 15 $\mu\text{g ml}^{-1}$ adiponectin or the indicated small-molecule compounds (10 μM). #, AdipoRon; ##, no. 112254; ###, no. 165073.



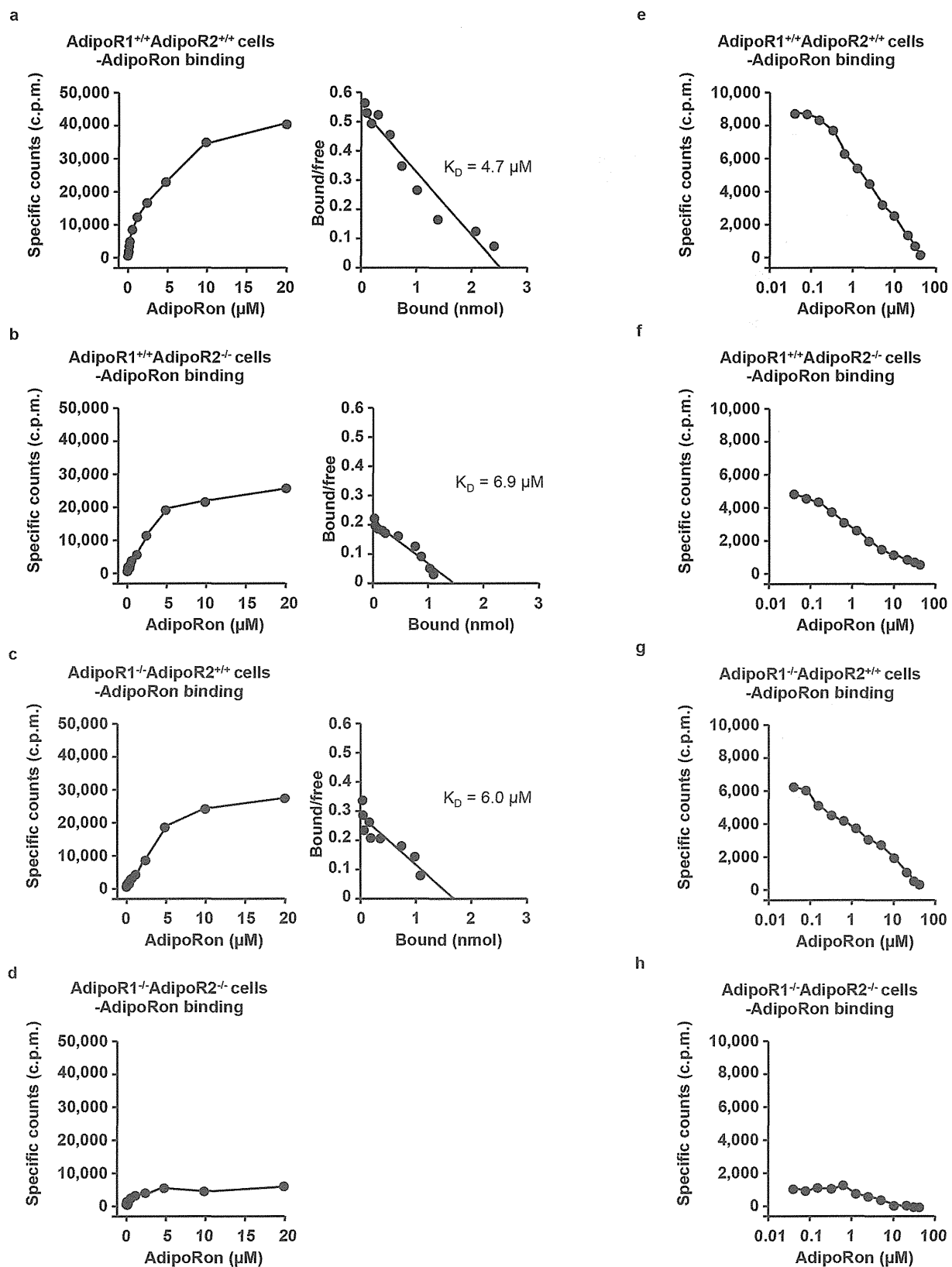
Extended Data Figure 2 | Distribution curves showing Z scores.

a. Distribution curve showing Z scores representing AMPK activity for all compounds tested in C2C12 myotubes shown in Extended Data Table 1 and Extended Data Fig. 1. The dashed line indicates the Z score cut-off for compounds scored as hits, which showed higher activity than 80% of that seen

with adiponectin. **b.** Distribution curve showing Z scores representing AdipoR dependency of AMPK activation for 39 compounds tested in C2C12 myotubes shown in Extended Data Table 2. Indicated are the location of AdipoRon, another hit (no. 112254), and non-hit (no. 165073).

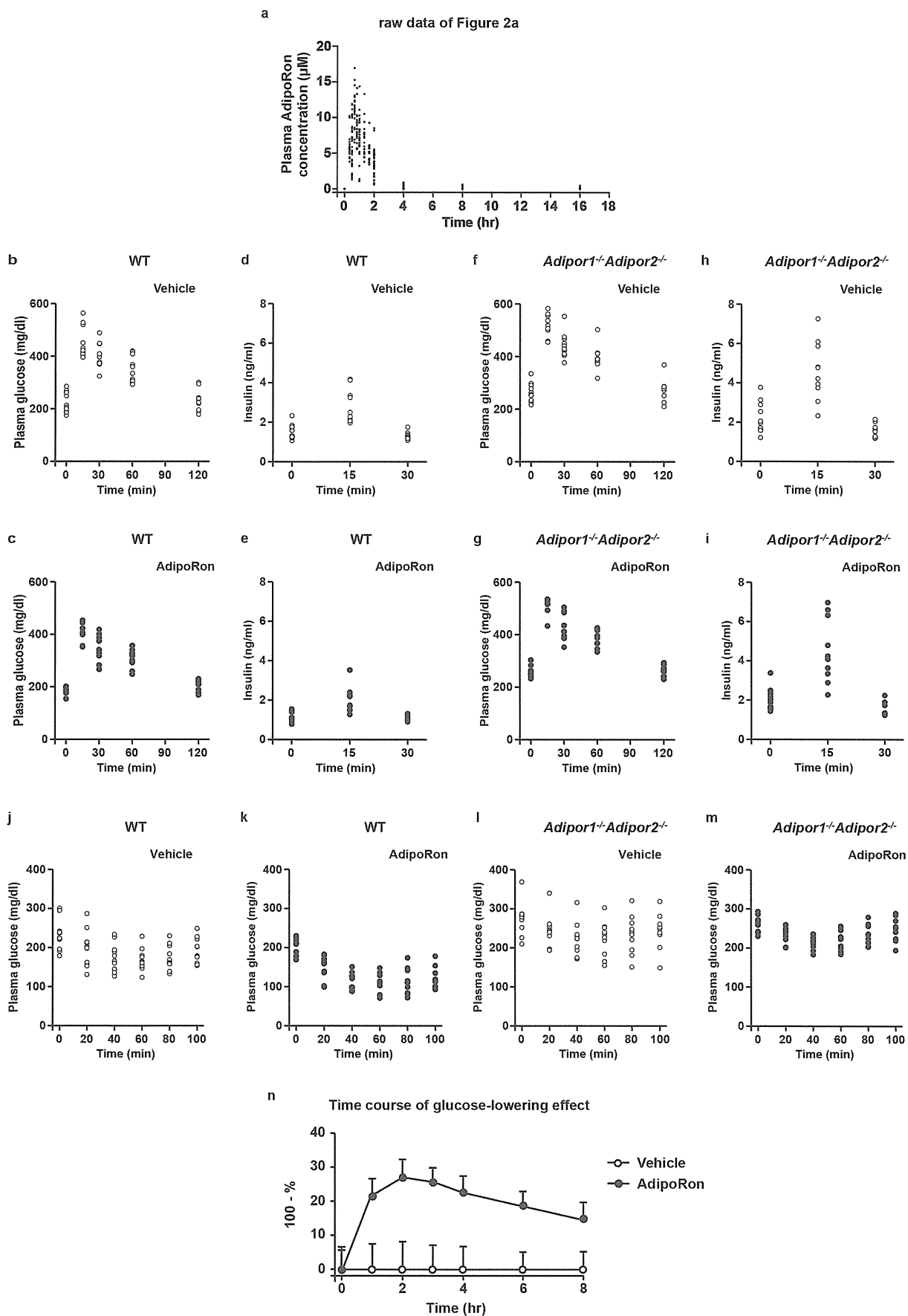


Extended Data Figure 3 | The effect of AdipoRon on complex I activity, and expression of *Adipor1* and *Adipor2* mRNA in C2C12 myotubes transfected with the indicated siRNA duplex. **a**, Complex I activities were measured with the indicated concentrations of rotenone or AdipoRon. **b**, **c**, *Adipor1* (**b**) and *Adipor2* (**c**) mRNA levels were analysed by RT-qPCR. All values are presented as mean \pm s.e.m. **a**, $n = 3-7$; **b**, **c**, $n = 3$ each; * $P < 0.05$ and ** $P < 0.01$ compared to control or unrelated siRNA cells. NS, not significant.



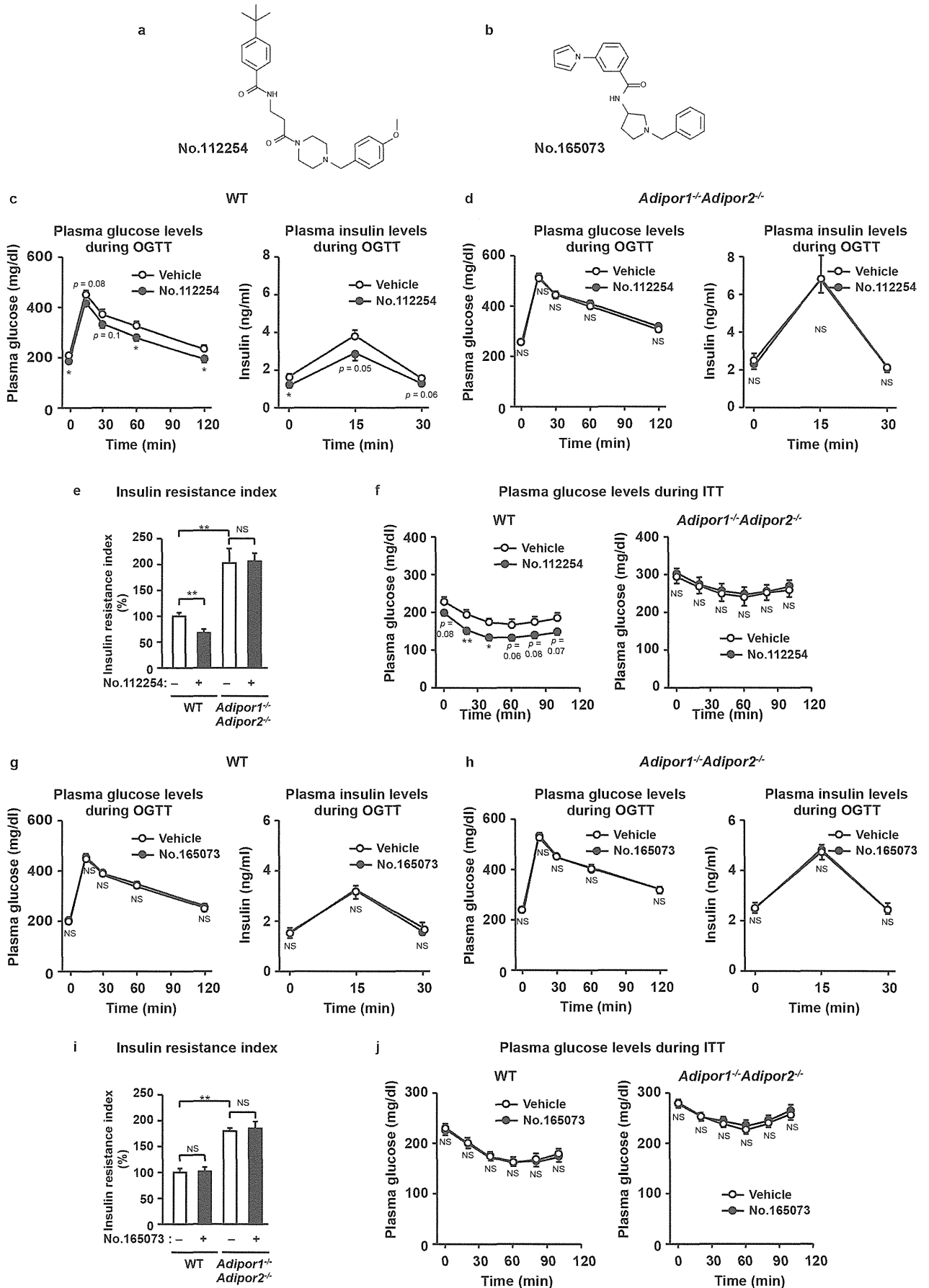
Extended Data Figure 4 | AdipoRon binding to AdipoR1 and AdipoR2. a–d, Binding and Scatchard analyses of [³H]AdipoRon to primary hepatocytes from wild-type (a), *Adipor2*^{-/-} knockout (b), *Adipor1*^{-/-} knockout (c) and *Adipor1*^{-/-} *Adipor2*^{-/-} double-knockout (d) mice. e–h, Concentration-dependent competitive [³H]AdipoRon binding to primary hepatocytes from

wild-type (e), *Adipor2*^{-/-} knockout (f), *Adipor1*^{-/-} knockout (g) and *Adipor1*^{-/-} *Adipor2*^{-/-} double-knockout (h) mice. Binding analyses were performed using the indicated concentrations of AdipoRon. c.p.m., counts per minute.



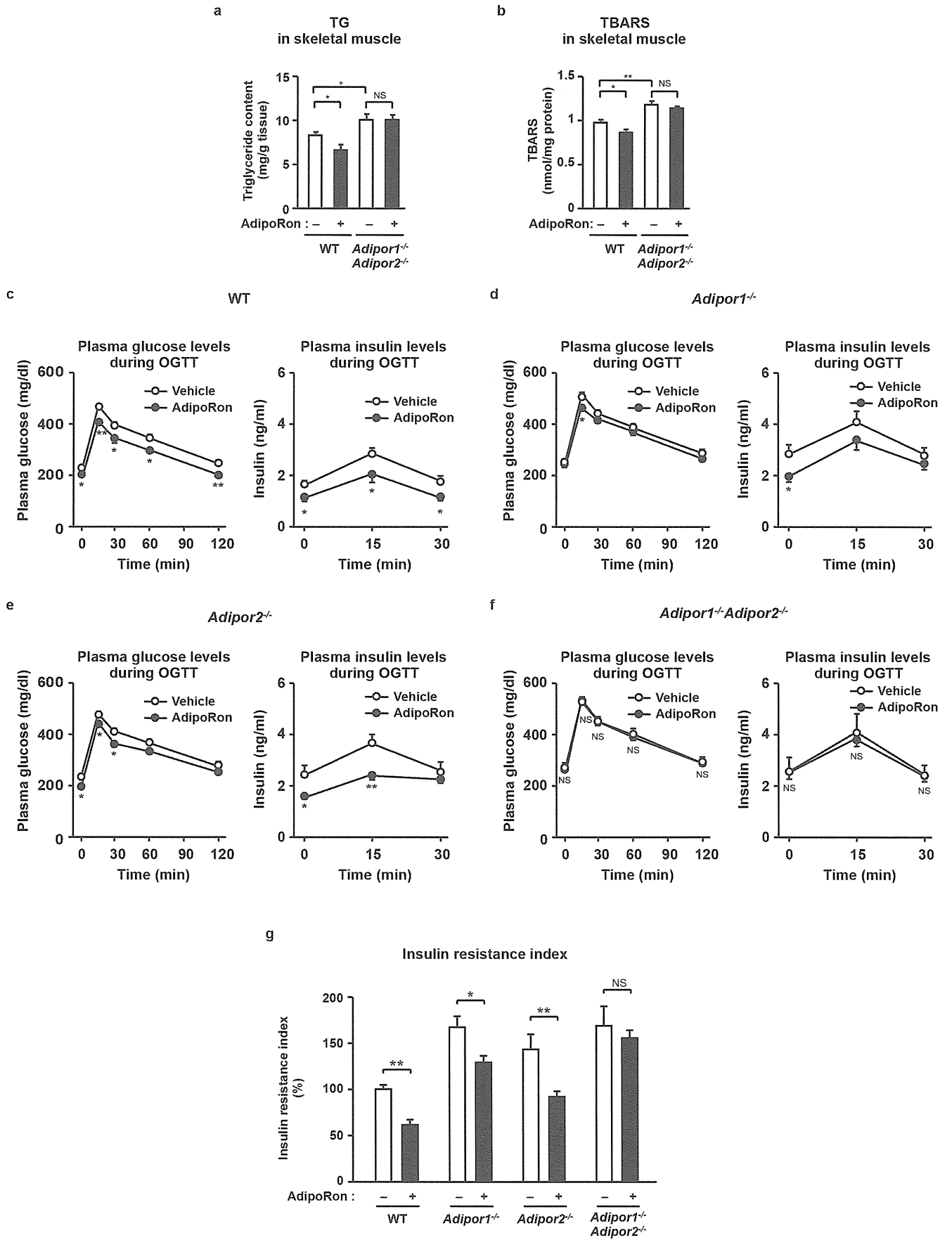
Extended Data Figure 5 | Raw data of Fig. 2 and time course of glucose-lowering effect of AdipoRon. **a–m**, Raw data of Fig. 2a (a), Fig. 2d, left (b, c), Fig. 2d, right (d, e), Fig. 2e, left (f, g), Fig. 2e, right (h, i), Fig. 2g, left (j, k) and Fig. 2g, right (l, m). **n**, Time course of glucose-lowering effect of

AdipoRon. Data are calculated from data in Fig. 4a. The glucose-lowering effect of AdipoRon was obtained by the following equation and expressed as %: $(\text{vehicle plasma glucose} - \text{AdipoRon plasma glucose}) / \text{vehicle plasma glucose}$. All values are presented as mean \pm s.e.m.



Extended Data Figure 6 | The effects of compounds 112254 and 165073 on insulin resistance and glucose intolerance via AdipoR. a, b, Chemical structures of compounds 112254 (a) and 165073 (b). c–j, Plasma glucose (c left, d left, f, g left, h left, j), plasma insulin (c right, d right, g right, h right) and insulin resistance index (e, i) during oral glucose tolerance test (OGTT) (1.0 g glucose per kg body weight) (c, d, g, h) or during insulin tolerance test

(ITT) (0.5 U insulin per kg body weight) (f, j), in wild-type and *Adipor1*^{-/-}*Adipor2*^{-/-} double-knockout mice, treated with or without compounds 112254 or 165073 (50 mg per kg body weight). All values are presented as mean ± s.e.m. c–f, *n* = 10 each; g–j, *n* = 7 each from 2, 3 independent experiments, **P* < 0.05 and ***P* < 0.01 compared to control or as indicated. NS, not significant.



Extended Data Figure 7 | The effects of AdipoRon on glucose metabolism in *Adipor1*^{-/-}, *Adipor2*^{-/-} and *Adipor1*^{-/-} *Adipor2*^{-/-} mice. a, Triglyceride content (a) and TBARS (b) in skeletal muscle from wild-type or *Adipor1*^{-/-} *Adipor2*^{-/-} double-knockout mice treated with or without AdipoRon (50 mg per kg body weight). c–g, The effects of AdipoRon on glucose metabolism in *Adipor1*^{-/-}, *Adipor2*^{-/-} and *Adipor1*^{-/-} *Adipor2*^{-/-} mice.

Plasma glucose (c–f, left panels), plasma insulin (c–f, right panels) and insulin resistance index (g) during oral glucose tolerance test (OGTT) (1.0 g glucose per kg body weight). All values are presented as mean ± s.e.m. a–d, f, n = 10 each; e, n = 7 each; g, n = 7–10; *P < 0.05 and **P < 0.01 compared to vehicle mice. NS, not significant.